Experimental Neurology 317 (2019) 155–167

Contents lists available at ScienceDirect

Experimental Neurology

journal homepage: www.elsevier.com/locate/yexnr

Research paper

Deep brain stimulation of the ventroanterior and ventrolateral thalamus improves motor function in a rat model of Parkinson's disease

Heidi R. Tucker[a], Emily Mahoney[a], Ashok Chhetri[a], Kristen Unger[a], Gianna Mamone[a], Gabrielle Kim[a], Aliyah Audil[a], Benjamin Moolick[a], Eric S. Molho[b], Julie G. Pilitsis[a,c], Damian S. Shin[a,b,*]

[a] Department of Neuroscience & Experimental Therapeutics, Albany Medical College, Albany, NY, United States of America
[b] Department of Neurology, Albany Medical Center, Albany, NY, United States of America
[c] Department of Neurosurgery, Albany Medical Center, Albany, NY, United States of America

ARTICLE INFO

Keywords:
6-hydroxydopamine
Neuromodulation
Hemiparkinsonian
Electrical stimulation
Forelimb akinesia
Whole-cell patch-clamp
Voa thalamus
Vop thalamus

ABSTRACT

Parkinson's disease (PD) is a neurodegenerative disease with affected individuals exhibiting motor symptoms of bradykinesia, muscle rigidity, tremor, postural instability and gait dysfunction. The current gold standard treatment is pharmacotherapy with levodopa, but long-term use is associated with motor response fluctuations and can cause abnormal movements called dyskinesias. An alternative treatment option is deep brain stimulation (DBS) with the two FDA-approved brain targets for PD situated in the basal ganglia; specifically, in the subthalamic nucleus (STN) and globus pallidus pars interna (GPi). Both improve quality of life and motor scores by ~50–70% in well-selected patients but can also elicit adverse effects on cognition and other non-motor symptoms. Therefore, identifying a novel DBS target that is efficacious for patients not optimally responsive to current DBS targets with fewer side-effects has clear clinical merit. Here, we investigate whether the ventroanterior (VA) and ventrolateral (VL) motor nuclei of the thalamus can serve as novel and effective DBS targets for PD. In the limb-use asymmetry test (LAT), hemiparkinsonian rats showcased left forelimb akinesia and touched only 6.5 ± 1.3% with that paw. However, these animals touched equally with both forepaws with DBS at 10 Hz, 100 μsec pulse width and 100 uA cathodic stimulation in the VA (n = 7), VL (n = 8) or at the interface between the two thalamic nuclei which we refer to as the VA|VL (n = 12). With whole-cell patch-clamp recordings, we noted that VA|VL stimulation in vitro increased the number of induced action potentials in proximal neurons in both areas albeit VL neurons transitioned from bursting to non-bursting action potentials (APs) with large excitatory postsynaptic potentials time-locked to stimulation. In contrast, VA neurons were excited with VA|VL electrical stimulation but with little change in spiking phenotype. Overall, our findings show that DBS in the VA, VL or VA|VL improved motor function in a rat model of PD; plausibly via increased excitation of residing neurons.

1. Introduction

Parkinson's Disease (PD) affects 1% of people over 60 years of age (Tysnes and Storstein, 2017) and coincides pathologically with the expression of Lewy bodies (Spillantini et al., 1998) and the loss of 50–70% of substantia nigra pars compacta (SNc) dopaminergic (DA) neurons at diagnosis (Chen et al., 2013). This neurodegenerative disease is clinically characterized by the classically described motor symptoms of bradykinesia, rigidity, resting tremor, reduced facial expression, postural instability and gait dysfunction (Postuma et al., 2015) although non-motor symptoms also impact quality of life. Currently, levodopa is considered the gold standard of treatment, but long-term use can lead to motor fluctuations and levodopa-induced dyskinesias which can be problematic (Fabbrini et al., 2007).

Deep brain stimulation (DBS) is a neuromodulatory approach involving electrical stimulation of subcortical brain structures to modulate neural function and network communication. At present, the two FDA-approved DBS targets for PD is the subthalamic nucleus (STN) and the globus pallidus par interna (GPi), which are two brain areas in the basal ganglia (BG) (Wichmann and Delong, 2011, 2016). Overall, this therapeutic approach improves motor scores in well-selected patients by 50–70%. Also, adverse cognitive effects including confusion and

* Corresponding author at: Department of Neuroscience & Experimental Therapeutics, Department of Neurology, Albany Medical College, Albany, NY 12208, USA.
E-mail address: shind@amc.edu (D.S. Shin).

https://doi.org/10.1016/j.expneurol.2019.03.008
Received 4 January 2019; Received in revised form 26 February 2019; Accepted 14 March 2019
Available online 16 March 2019
0014-4886/

impaired decision-making have been noted with DBS albeit rates are low (Buhmann et al., 2017). Patients may also experience paresthesia and dysarthria. Therefore, identifying a novel DBS target that provides improvement for patients not optimally responsive to current targets, fewer side-effects and/or greater efficacy has clinical utility.

In search of potential new anatomical sites for DBS, the box-and-arrow diagram describes the BG circuitry (Albin et al., 1989; DeLong, 1990) in a simplistic manner, but still serves as an excellent resource tool and initial working framework to describe BG network communication circuitry and PD pathophysiology. In this model, it is notable that the ventroanterior (VA) and ventrolateral (VL) motor thalamic areas are critically positioned between the output of the BG (e.g., GPi), cerebellum and motor-related cortices and intuitively seems to be an ideal candidate for neuromodulation for improving motor function. The human VA and rostral VL thalamus is homologous in rats to the VA thalamus and ventroanterior oralis/ventroposterior oralis (Voa-Vop) according to the Hassler classification (Hassler, 1950; Hassler et al., 1979) or the VA thalamus and ventrolateral anterior nucleus (VLa) using the Jones classification (Macchi and Jones, 1997). For simplicity, we employ Hassler's nomenclature and refer to these areas in the rat brain as homologous to the human "VA and Voa-Vop". Interestingly, these motor thalamic nuclei have largely been overlooked as a novel DBS target for PD despite its key involvement in motor function with sparse limbic connectivity. The latter point is notable since adverse effects concerning cognitive impairment and/or depression may be less likely to occur from neuromodulation of these areas.

While we aim to be the first to examine whether DBS in the VA and VL improves motor function in a rat model of PD, there have been indications elsewhere that neuromodulating these thalamic nuclei can improve motor function. Specifically, it was reported that optogenetic theta burst stimulation of the VA thalamus in a haloperidol rat model of PD improved akinesia and exploratory behavior (Seeger-Armbruster et al., 2015). In patients with dystonia, DBS at 130 Hz of the Voa/VLa thalamus reduced head tremor by 78% and dystonia by 70% (Pauls et al., 2014). Together, these studies suggest that neuromodulating the VA and/or VL thalamus can affect a range of motor symptoms ranging from akinesia to dystonia and tremor. Therefore, in this study, we investigated whether DBS in a rat model of PD improves motor function.

2. Materials and methods

2.1. Animals and surgeries

All animal use in our study complied with the National Institutes of Health and Albany Medical College (AMC) Institutional Animal Care and Use Committee (IACUC) guidelines. Animals were purchased from Charles River (Wilmington, MA, USA) or Taconic (Germantown, NY, USA) and all procedures were performed during the light phase of the light-dark cycle (7:00 AM to 7:00 PM, lights on). We provide a general scheme depicting the timeline of craniotomy surgery, animal behavior testing to assess forelimb akinesia and the electrical stimulation paradigm in Fig. 1A.

Male Sprague Dawley rats weighing 225–550 g were anesthetized with 1–3% isoflurane using an inhalant system (Harvard Apparatus, MA, USA). Twenty minutes prior to craniotomy surgery, rats were injected intraperitoneal (IP) with pargyline (50 mg/kg) and desipramine HCl (25 mg/kg) to inhibit monoamine oxidase B activity and noradrenergic reuptake transporters, respectively. Lidocaine jelly (Akorn Pharmaceutics, Lake Forest, IL, USA) was applied to ear bars, the top of the head was shaved and the animal placed in a stereotaxic frame (David Kopf Instruments, CA, USA). Body temperature was maintained at 37 °C during surgery with a warming blanket with feedback control (Homeothermic monitor, Harvard Apparatus, MA, USA). Lubifresh P.M. (Major Pharmaceuticals, Livonia, MI, USA) was applied to the eyes to prevent dryness. Bupivicaine (100 µl) (Cardinal Health, Dublin, OH, USA) was injected subcutaneously (subQ) at the incision site.

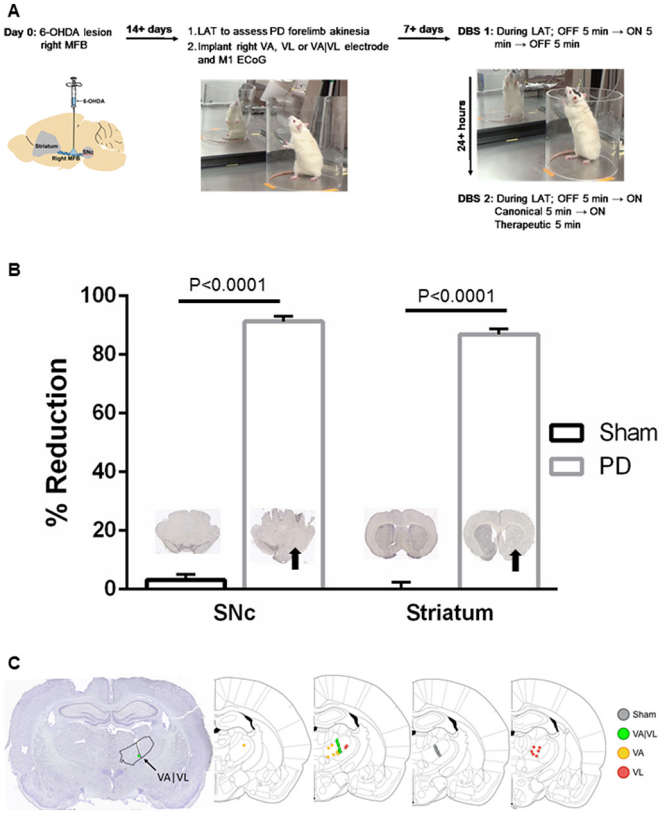

Fig. 1. (A) Timeline depicts when craniotomy surgery, LAT and DBS was tested. Canonical stimulation involves 150 Hz, 60 µsec pulse width and 400 µA current amplitude, which are settings used in preclinical studies for STN-DBS. Conversely, therapeutic stimulation was most often at 10 Hz, 100 µsec pulse width and 100 µA current amplitude (derived mode values). (B) Relative intensity of right hemisphere TH staining compared to left (% reduction) was quantified in the SNc and striatum of PD and sham rats. Representative TH immuno-stained slices are shown with black arrows denoting hemisphere with loss of TH expression. (C) Sample CV stained slice with outline of thalamus (black dashed line) and location of electrode tip (green dot). Dots show tip placement of stimulating electrodes: VA|VL (green), VA (yellow), VL (red) and Sham (gray). (For interpretation of the references to colour in this figure legend, the reader is referred to the web version of this article.)

We generated hemiparkinsonian rats as before and injected 4.5 µl of 6-hydroxydopamine (6-OHDA: 3 µg/µl) made up with 0.1% ascorbic acid in 0.9% NaCl saline (Sigma-Aldrich, St. Louis, MO, USA) (O'Connor et al., 2016; 2017; Phookan et al., 2015; Sutton et al., 2015; 2013a). This was done in the right medial forebrain bundle (MFB) (from bregma: 4.4 mm posterior, 1.5 mm lateral and 7.5 mm ventral from dura) via a 10 µl injection syringe (Hamilton Company, Reno, NV, USA) at a rate of 0.5 µl/min to degenerate dopaminergic neurons in the right SNc and their efferent outputs to the striatum. In contrast, sham animals received a 4.5 µl injection of vehicle control (0.1% ascorbic acid in 0.9% NaCl saline). Topical antibiotic ointment was applied on the incision following closure with surgical staples and animals were administered buprenorphine (subQ: 0.12 g/kg) immediately after craniotomy surgery and ~ every 12 h for 48 h after surgery. Alternately some rats received buprenorphine once immediately after surgery and were provided with one Rimadyl (2 mg) tablet (Bio-Serv, Flemington, NJ, USA) each day for two consecutive days for post-surgical pain management.

Two weeks later, hemiparkinsonian phenotype was confirmed using the limb-use asymmetry test (LAT) (Schallert et al., 2000) as described previously (Sutton et al., 2013b). Here, animals were placed in a transparent cylinder and videotaped for 5 min with rats touching a minimum 15–20 times. The forepaw touches were then quantified as

A

Session	Target			
	Sham	VA	VL	VA|VL
No DBS	10	7	8	12
DBS 1	0	7	8	11
DBS 2	0	5	7	9

B

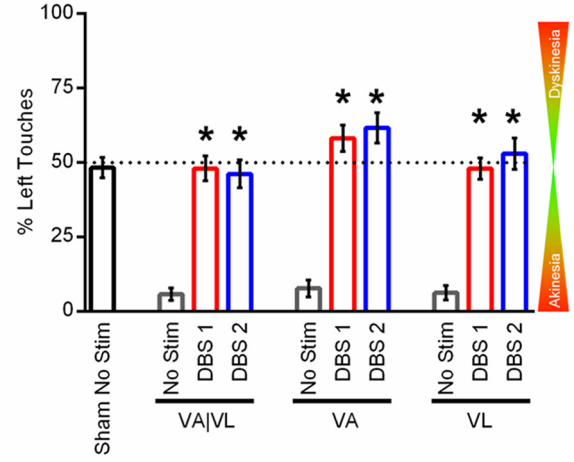

Fig. 2. (A) A summary of the animal sample size implanted with VA, VL or VA|VL DBS stimulating electrodes while undertaking the LAT. 'No DBS' group are PD rats with stimulating electrodes, but without stimulation. Sham animals are non-PD rats with a stimulating electrode implanted at the interface area between the VA and VL (denoted as 'VA|VL'), but without electrical stimulation. (B) Sham rats exhibited normal forelimb function with their left forepaw. PD rats implanted either in the VA|VL, VA or in the VL but without electrical stimulation exhibited marked left forelimb akinesia by touching < 20% with their left forepaw. Mode stimulation settings for PD animals were 10 Hz, 100 μsec pulse width and 100 μA current amplitude. Regardless of the specific targeted motor thalamic area, DBS significantly increased left forepaw touches on day 1 and day 2, making them statistically similar to sham animals.

number of left contacts/number of total contacts x 100. Hemiparkinsonian rats touching < 20% with left impaired forepaw were denoted as displaying forelimb akinesia (Schallert et al., 2000).

For DBS electrode implantation, animals were anesthetized and prepped for craniotomy surgery as described above. A stainless steel twisted wire electrode (125 μm diameter for each of two wires, bundled together for a total diameter approximately 350 μm,12 mm long, Plastics One, Roanoke VA, USA) was implanted unilaterally in the right hemisphere in the VA and VL nuclei, which is denoted in the rat atlas (Paxinos and Watson, 1996) and also in the un-delineated border area or interface region between these regions (VA|VL). For the VA|VL, we implant from bregma: 2.1 mm posterior, 1.8 mm lateral and 5.4 mm ventral from dura (n = 12); for the VA; we implant from bregma: 1.9 mm posterior, 1.8 mm lateral and 5.7 mm ventral from dura (n = 7); and for the VL, we implant from bregma: 2.3 mm posterior, 1.7 mm lateral and 5.7 mm ventral from dura (n = 8). As a control group, sham rats received DBS electrodes only in the VA|VL in the right hemisphere (n = 10) (Fig. 2A). In addition, all animals had a screw electrode implanted in the right primary motor cortex (M1) (from bregma: 1.6 mm anterior, 3.0 mm lateral, and 2.0 mm ventral from dura) to obtain electrocorticograms (ECoGs) with a reference screw electrode placed in the midline in the nasal bone. Stimulating and recording electrodes were placed inside a cap pedestal (Plastics one, Roanoke VA, USA) and this, along with anchor screws, were held in position with glue and dental cement (Duralay Reliance Dental, IL, USA). Post-operative care and analgesic pain management were the same as above.

2.2. Electrical stimulation

Animals with dental cement-covered implants were tethered to a commutator with connecting cables to allow electrical stimulation during LAT testing. Stimulation was applied using a Grass S88 Stimulator coupled to a PSIU-6 current isolation unit (Grass Products, Natus Neurology, Warwick, RI, USA) with a range of frequencies, pulse widths, cathodic vs. anodal stimulation and current amplitudes. Animals were placed in the plexiglass cylinder and recorded for 5 min without DBS prior to receiving stimulation and with DBS turned off for 5 min following stimulation for the "DBS 1" protocol. Alternately, animals were placed in the plexiglass cylinder and recorded for 5 min without DBS, then for 5 min with DBS set to canonical DBS settings for PD in the STN or GPi at 150 Hz, 60 μs and 400 μA and for 5 min with optimal thalamic DBS settings for 5 min for the "DBS 2" protocol.

To find the optimal current amplitude settings for each animal, we first elicited abnormal forelimb movements with electrical stimulation, which we denote as dyskinesia and then reduced amplitudes until rats were observed to touch with both forepaws in the LAT. This was done qualitatively as a quick screening process rather than employ the abnormal involuntary motor score (AIMS) (Lundblad et al., 2002). Notably, eliciting abnormal motor movement in PD patients from DBS contacts in the clinic is similarly done as part of the stimulation amplitude optimization process (*pers comms*, AMC movement disorders clinic).

2.3. Tyrosine hydroxylase immunostaining

As elsewhere, rats were transcardiac-perfused with 4% paraformaldehyde (PFA) after the completion of the experiment (O'Connor et al., 2016; 2017; Phookan et al., 2015; Sutton et al., 2015; 2013a). Brains were extracted, placed in 4% PFA before being placed in 30% sucrose to cryoprotect the brain and then sectioned at 60 μm to obtain slices containing the striatum and substantia nigra (SNc) using a cryostat (HM500M, Leica Biosystems Inc., IL, USA). Slices were then incubated in 3% H_2O_2 for 10 min to 1 h and in 0.1 M PBS (3-6× for 10 min each) and incubated overnight in normal goat serum with 0.1 M PBS at 4 °C. Slices were then incubated in anti-tyrosine hydroxylase (TH) primary antibody (1:500, Novus Biologicals; CAT# NB300–109) for 24–48 h and subsequently washed and incubated in secondary peroxidase-conjugated goat-anti-rabbit secondary antibody (1:500) (Sigma; CAT# 45-A0545). The tissue was washed 3-6× for 10 min in 0.1 M PBS and in DAB for chemo-reaction, then 2× in 0.1 M PBS. After, slices were mounted on gelatin-coated slides (Superfrost Gold Plus, Fisher Scientific, Pittsburgh, PA) and cover slipped with CytoSeal (Thermo Scientific/Richard-Allan Scientific). TH immuno-stained slides were scanned with PathScan Enabler IV (Electron Microscopy Sciences, Hatfield, PA) and later pixilated using ImageJ software (ver 2.1.4.7, NIH, MD) and the density of TH pixilation on the right lesioned striatum and SNc was compared to its left un-lesioned side to determine the extent of dopaminergic cell body and axonal degeneration, respectively, and represented as a percent reduction of TH immunostaining.

2.4. Nissl cresyl violet staining

Electrode placement was confirmed in all rats by taking brain sections and staining for nissl substance with Cresyl violet (CV) as described elsewhere (O'Connor et al., 2016; 2017; Phookan et al., 2015; Sutton et al., 2015; 2013a). In brief, cut frozen sections 60 μm thick were rehydrated with 95% ethanol (ETOH) for 10 min followed by 3 subsequent washes in 70% ETOH, 40% ETOH and distilled water for 3 min in each solution. Slides were then stained in CV followed by a

dehydration process involving a 3 min de-stain in distilled water with acetic acid, 2 min incubations in 40% ETOH, 70% ETOH and 95% ETOH and a 3 min incubation in 100% ETOH. Slides were then placed in 100% Xylene for 3 min before being cover-slipped with CytoSeal (Thermo Scientific/Richard-Allan Scientific). CV stained slides were then imaged using the PathScan Enabler IV (Electron Microscopy Sciences, Hatfield, PA). Images were co-registered to a rat atlas to determine electrode location.

2.5. Chemicals and drugs

All chemicals were purchased from Sigma Aldrich (St. Louis, MO, USA) whereas items for immunohistochemistry such as antibodies were purchased from Santa Cruz Biotechnology (CA, USA), Novus Biologicals (Littleton, CO, USA) or Jackson ImmunoResearch Laboratories (West Grove, PA, USA).

2.6. In vitro whole-cell patch-clamp & in vivo eCoG recordings

We follow procedures as we have done elsewhere (Shin and Carlen, 2008; Shin et al., 2007; Yu et al., 2016). Briefly, a total of 16 naive rat pups between postnatal days 11–16 were quickly sacrificed using a guillotine and two to three brain slices 400 μm thick were obtained from each hemisphere in the coronal orientation with a vibratome VT 1200S (Leica, IL, USA) in dissecting solution containing (in mM): 87 NaCl, 2.5 KCl, 1.25 NaH2PO4, 7 MgCl2, 0.5 CaCl2, 24 NaHCO3, 25 glucose and 75 sucrose (oxygenated with carbogen at 95% O2/ 5% CO2). After, slices were placed in an incubation chamber (Automate Scientific, Berkeley, CA, USA) for 1 h at room temperature in oxygenated artificial cerebrospinal fluid (aCSF) containing (in mM): 125 NaCl, 2.5 KCl, 1 MgCl2, 1.25 NaH2PO4, 1 CaCl2, 25 NaHCO3, and 10 glucose at pH 7.4, heated to 34 °C. For recordings, a brain slice was placed in a RC-26 recording chamber (Warner Instruments, Hamden, CT, USA) and a 125 μm shaft diameter stimulating biconcentric electrode (FHC, ME, USA) was positioned in the VA|VL at a distance < 150 μm from the recorded VA or VL neuron and connected to a stimulator (Grass SD9 stimulator, Natus Neurology Inc., MA, USA). Cells were viewed under infrared differential interference contrast (IR-DIC) imaging using an Olympus BX51WI upright microscope (Olympus Optical, NY, USA) equipped with a 40× water immersion lens. Whole-cell patch-clamp electrodes were pulled from borosilicate capillaries (World Precision Instruments, FL, USA) to a pipette tip resistance of 5–8 MΩ and filled with intracellular solution containing (in mM): 110 K-gluconate, 8 NaCl, 20 KCl, 1 MgCl2, 0.0001 CaCl2, 10 Na- HEPES, 2 Na-ATP, 0.3 Na-GTP, pH of 7.4.

After whole-cell patch-clamp configuration was achieved, a 5 min baseline was obtained prior to a 5 min monophasic bipolar and cathodic voltage stimulation at 10 Hz, 100 μsec pulse width at 1 V and then 2 V and lastly for 5 min at 3 V stimulation in sequence for each recorded neuron. These voltage stimulations are consistent with those used by others to elucidate effects of DBS on neural activity in in vitro studies (Garcia et al., 2003).

To help delineate effects of VA|VL stimulation on VA and VL neuronal membrane properties and excitability, we applied a current-voltage (I-V) stimulation paradigm (referred to as an “evoked response”) and injected positive and negative current in 50 pA square steps lasting 900 msec via the pipette electrode to depolarize and hyperpolarize the recorded neuron, respectively. This was done between every 5 min recording and stimulation period when spontaneous activity was monitored in the current-clamp mode set to 0 current to view changes in resting membrane potential and post-synaptic potentials. Afterwards, a 10 min post-stimulation recording was obtained in current-clamp mode followed by a final I-V evoked response.

Whole-cell patch-clamp recordings were obtained using an Axopatch 200B amplifier and 1322A digitizer (Molecular Devices, CA, USA), which was low-pass filtered at 5 kHz and sampled at 10 kHz. Only one neuron was recorded from stimulated slices. Multiple recordings were obtained from unstimulated slices.

With our ECoG electrode recordings, local field potentials (LFPs) were obtained from the primary motor cortex (M1) in the differential configuration (Model 3000, A-M Systems, WA, USA). Signals were sampled at 1 kHz, high- and low-passed at 1 Hz and 300 Hz, respectively, and digitized (MiniDigi 1B, Molecular Devices, CA, USA) while rats were in the plexiglass cylinder performing the LAT. The spectrogram analyses compared % of total power spectral densities (PSD) at each frequency domain before, during and after VA|VL DBS and shown with the same Y axis to allow for direct comparison of representative power spectra. Frequency domains were as follows: delta (0–4 Hz), theta (4–7 Hz), alpha (8–12 Hz), beta (12–30 Hz) and gamma (> 30 Hz) and viewed with a 1 min window prior to and during VA|VL DBS. Analysis was not performed from time windows where stimulation (blue arrows, Fig. 7B) and harmonics (red arrows, Fig. 7B) were present except at alpha frequencies, where stimulation at 10 Hz can encompass all or most of the frequency domain. In this case, the power in alpha frequencies presumably increased due to stimulation artifacts. Each PD rat underwent two DBS repeated trials (DBS 1 and DBS 2) with improved forelimb function in the LAT and characterized as a percentage of combined trials for all animals having increased, decreased or no change for PSDs at each frequency domain in the M1 cortex with DBS as compared to without DBS.

2.7. Data analysis and statistics

We characterized VA and VL neurons having evoked burst action potentials (APs) when the time between the first and second APs with positive current injection was < 15 msec (Fig. 3Ai, bottom trace; Fig. 3Aii), which is within range of others (DeBusk et al., 1997; Escola et al., 2011; Tritsch et al., 2010; Wijesinghe et al., 2013). If a second AP was observed after this time window, the neuron was deemed as exhibiting non-burst APs (Fig. 3Ai, top trace).

Parametric data were analyzed by one-way ANOVA whereas non-parametric data involving pie-charts were done with a Fisher's exact test (Graphpad Prism 6, Version 6.0, LaJolla, CA, USA). For analyses involving changes in APs at 100 pA positive current injection with or without VA|VL electrical stimulation, we conducted an unpaired two-tailed *t*-test. For all statistical analyses, the data were considered significant at $p < 0.05$. TH immuno-stain data were analyzed by 2-way ANOVA.

3. Results

3.1. Histological verification of parkinsonian phenotype and electrode placement

TH immuno-staining in the striatum and SNc were used as proxy for degeneration of dopaminergic axons and cell bodies, respectively. Hemiparkinsonian phenotype in LAT was verified by TH immunostaining of the SNc, the striatum or both for all rats except for two animals (n = 1 VA and n = 1 VA|VL) where immuno-TH measurements could not be obtained. As comparison, TH immuno-staining was assessed from a subset of sham-lesioned rats. Relative intensity of TH staining in the right hemisphere SNc (n = 20) was reduced 91.3 ± 1.8% compared to the left non-lesioned SNc in hemiparkinsonian “PD” animals and only 3.2 ± 1.8% in sham rats (n = 7). Similarly, TH staining in the right hemisphere striatum (n = 12) was reduced 86.9 ± 1.8% compared to the left non-lesioned striatum in PD animals, but only −0.2 ± 2.4% was seen in sham animals (n = 7). In both the SNc and the striatum, PD animals had more marked loss in TH expression compared to the control sham group ($p < 0.0001$) (Fig. 1B). In addition to TH immunostaining, other brain slices were stained with CV and only animals with electrode locations confirmed in the VA|VL (green for PD and gray for sham), VA (yellow) or VL (red)

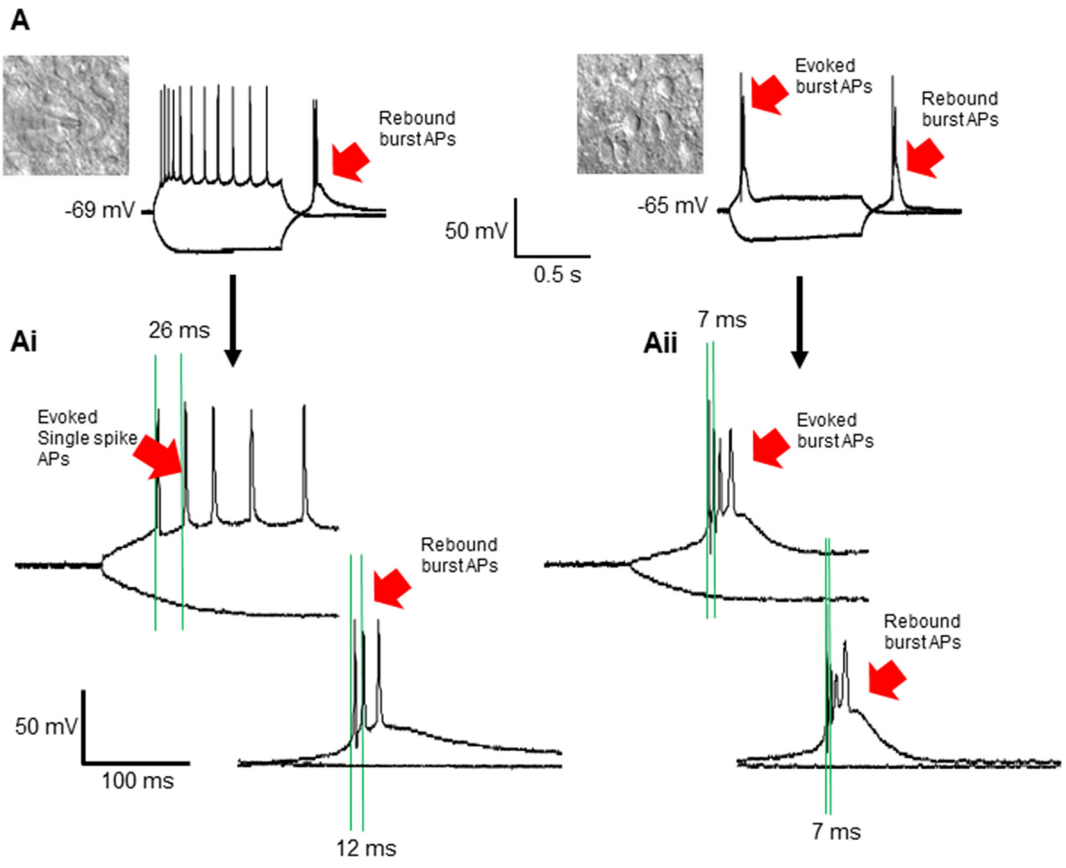

B

Neuronal Type	Sample size (total of 15 rats)	Resting membrane potential (mV)	Input resistance (mΩ)	Rebound bursts APs	Evoked burst APs	Both rebound & evoked burst APs
Ventroanterior (VA)	22 cells	-69.7 ± 1.1	331.6 ± 20.1	45.5%	54.5%	13.6%
Ventrolateral (VL)	18 cells	-65.4 ± 1.3 *(p=0.01)	212.3 ± 13.4 *(p<0.0001)	55.6% (N.S)	83.3% #(p=0.053)	38.9% #(p=0.067)

Fig. 3. (A) VA neuron (A) or VL neuron under IR-DIC with rebound or evoked burst action potentials (APs) denoted by red arrows in the current-voltage traces. Spiking activity induced with 100 pA positive current injected via the whole-cell patch-clamp recording electrode. Scale bar represents both VA and VL neuronal traces. (Ai) Traces are expanded from VA neurons in (A) to highlight induced single spiking waveforms and burst rebound APs. Conversely (Aii) are expanded views from the VL neuron from (A) to underscore the induced and rebound burst AP waveforms. For both expansions, the green vertical line is used in the Clampfit software program to derive the time between the start of the first and second APs with four sample times (in ms) provided. Summary of resting membrane potential and input resistance shown in (C). Data was analyzed by unpaired 2-way *t*-test between cell types with significance denoted with asterisks. (For interpretation of the references to colour in this figure legend, the reader is referred to the web version of this article.)

thalamic nuclei were included in the study (Fig. 1C).

3.2. VA, VL or VA|VL DBS improves forelimb akinesia in PD rats

Initially, we performed a first-pass optimization experiment in PD rats implanted on the right side with DBS electrodes in the VA (n = 1), VL (n = 1) or VA|VL (n = 2) to derive the optimal DBS settings for improving motor function using different frequencies, pulse widths, current amplitudes, anodal vs. cathodic stimulation. We noted that cathodic monophasic bipolar stimulation at 10 Hz, 100 μsec pulse width and 100 μA reduced forelimb akinesia. We then used these stimulation settings in a more expansive group of PD rats (Fig. 2A).

Prior to DBS, PD rats with stimulating electrode in the VA touched 7.8 ± 2.9% (n = 7), rats with an electrode in the VL touched 6.3 ± 2.5% (n = 8) and rats with the electrode in the VA|VL touched 5.8 ± 2.1% (n = 12) with their impaired left forepaw, all of which were significantly less than sham animals that touched 48.3 ± 3.1% (n = 10, $p < 0.0001$ for all targets). In contrast, PD rats with DBS in the VA touched 58.2 ± 4.5% during DBS 1 (n = 7) and 61.7 ± 5.1% during DBS 2 (n = 5), a significant improvement from rats not receiving DBS ($p < 0.0001$ for all targets). PD rats that received DBS in the VL touched 48 ± 3.6% during DBS 1 (n = 8) and 53 ± 5.3% during DBS 2 (n = 7), also a significant improvement compared to rats without DBS ($p < 0.0001$ for all targets). PD rats that received DBS at the VA|VL touched 48.1 ± 4.2% during DBS 1 (n = 11) and 46.2 ± 4.6% during DBS 2 (n = 9), which were significantly more left forelimb paw touches than rats without DBS ($p < 0.0001$ for all targets). PD rats that received DBS displayed improved forelimb function similar to sham animals (n = 10, $p > 0.05$) regardless of the motor thalamic area that was stimulated (Fig. 2B). No significant difference between DBS 1 and

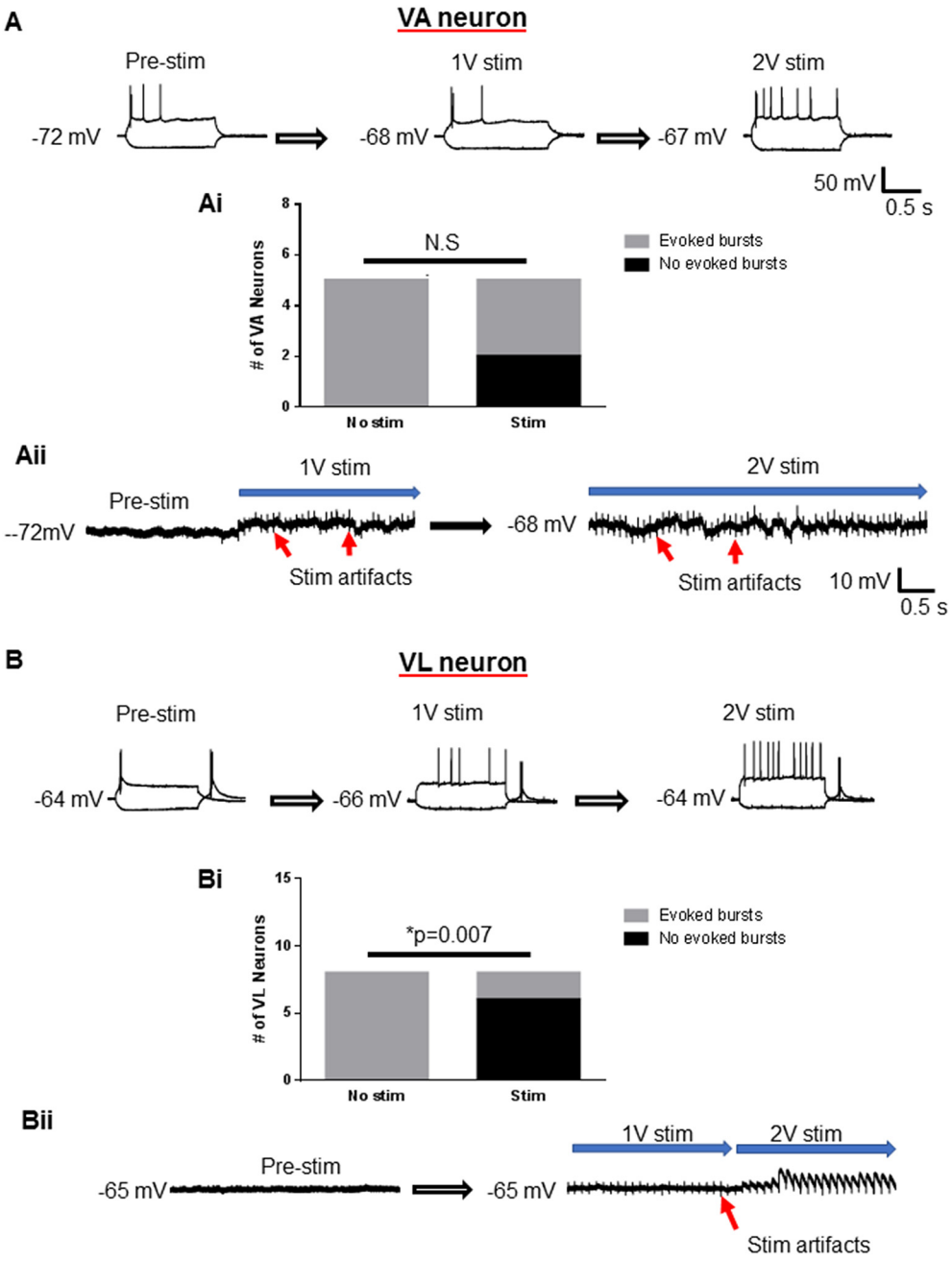

Fig. 4. (A) Raw traces from VA neurons without stimulation (pre-stim) or with 1 V and 2 V stimulation increased spiking frequency but not pattern, which is shown as compiled data of the number of VA neurons exhibiting evoked burst action potentials with and without stimulation. Data was analyzed using 2-sided Fisher's exact test. (Ai). In (Aii), stimulation (seen as artifacts in the traces) caused only minor fluctuations in resting membrane potential regardless of the voltage. In (B), raw traces from VL neurons are shown without stimulation (pre-stim) or 1 V and 2 V stimulation. Notably, this caused transition from evoked burst APs to many single spikes. Compiled data of the number of VL neurons with evoked action potentials with and without stimulation is shown in (Bi). Data was analyzed using 2-sided Fisher's exact test. In (Bii), stimulation (seen as artifacts in the traces) evoked large depolarizing potentials at higher voltages.

DBS 2 ($p > 0.05$ for all targets) shows retention of responsiveness to stimulation.

3.3. VA and VL neurons differ in resting membrane potential and response to VA|VL stimulation in vitro

We recorded from a total of 22 VA neurons and 18 VL neurons from 15 animals (Fig. 3A, B). VA neurons had a more hyperpolarized resting membrane potential (-69.7 ± 1.1 mV) than VL neurons (-65.4 ± 1.3 mV, $p = 0.01$) and higher membrane input resistance (VA: 331.6 ± 20.1 mΩ; VL: 212.3 ± 13.4 mΩ, $p < 0.0001$). With termination of negative current injection, both thalamic neurons had similar rebound burst APs (Fig. 3B). In response to positive current injection, there was a trend towards a higher proportion of VL neurons exhibiting evoked burst APs ($p = 0.053$) and having both rebound and evoked burst APs ($p = 0.067$) than VA neurons (Fig. 3B).

Without stimulation, most VA neurons exhibited a slight decrease in AP numbers induced by 100 pA positive current over time ($n = 13$ cells, $p = 0.389$, Fig. 5A). Yet, with electrical stimulation in the VA|VL region, VA neuronal excitability increased in a voltage-dependent manner (Figs. 4 & 5). Specifically, 1 V stimulation did not alter excitability ($n = 9$ cells, $p = 0.04$, Fig. 5A) but stimulation at 2 V caused 3.2 ± 2.0 more APs per cell with 100 pA positive current injection ($n = 10$ cells, $p = 0.033$, Fig. 5B) with a greater proportion of the neurons with increased spiking activity ($p = 0.036$, Fig. 5B). Similarly, 3 V stimulation in the VA|VL area elicited 1.6 ± 0.7 more APs per cell ($n = 9$ cells, $p = 0.006$) and a higher proportion of cells with increased spiking phenotype ($p = 0.028$, Fig. 5C). The changes in excitability were not associated with any alteration in resting membrane potential or input resistance with VA|VL stimulation at any voltage stimulation (data not show). Furthermore, we observed that VA neurons that exhibited evoked burst APs prior to stimulation still had evoked burst APs after VA|VL stimulation (Fig. 4Ai). In passive current clamp mode viewing, VA|VL stimulation had no marked effect on spontaneous activity with

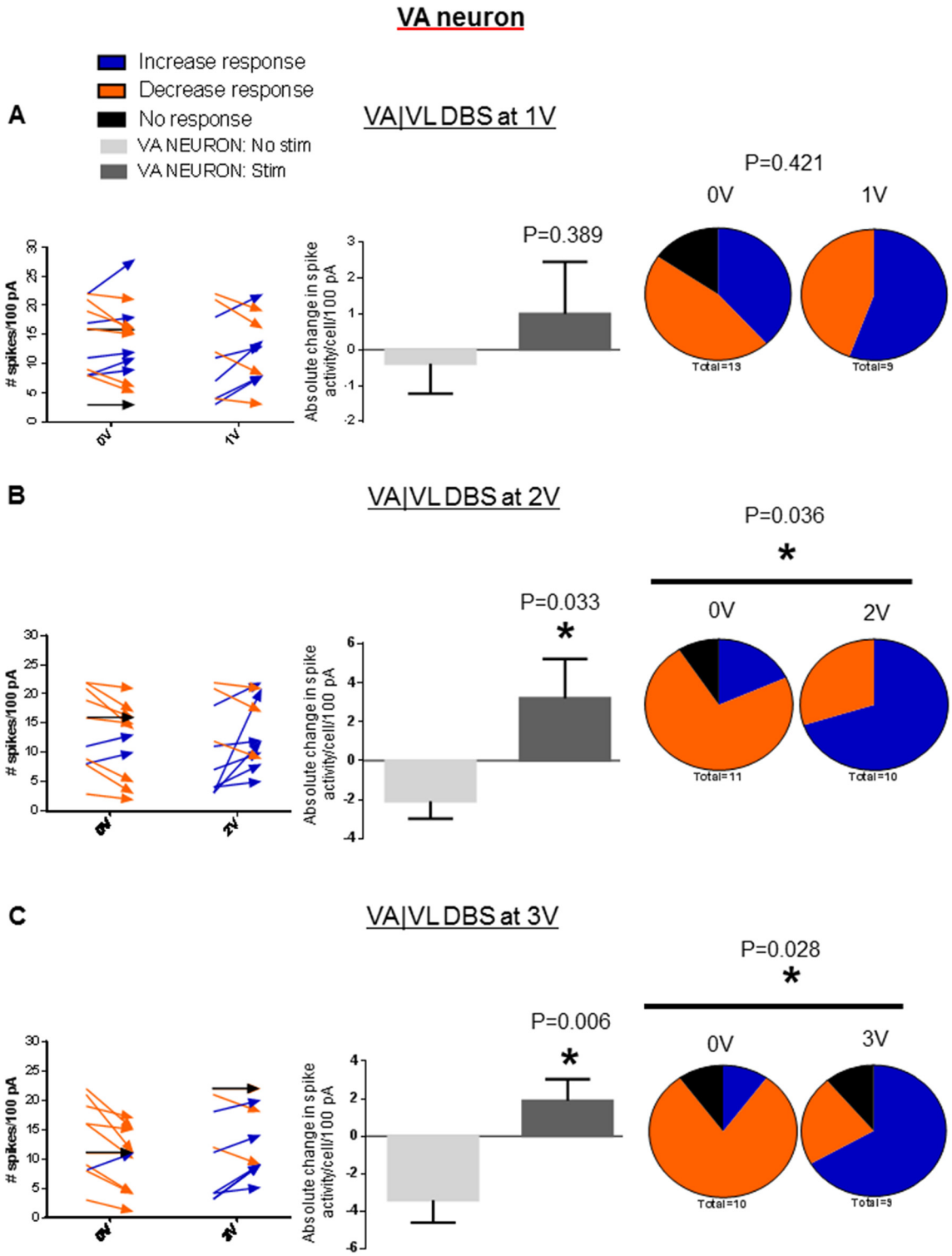

Fig. 5. Spiking activity of VA thalamic neurons before and during 1 V (A), 2 V (B), 3 V (C) stimulation at the VA|VL. Data shown for spikes elicited with 100 pA positive current injection. Beginning of arrows represent evoked response at baseline relative to endpoint, representing evoked response following 5 min baseline (0 V) or baseline plus 5 min stimulation (1, 2 or 3 V). The coinciding percentage change in the direction of the neuronal activity is shown as pie charts on the right with orange, blue and black denoting a decrease, increase or no change in spiking activity with stimulation, respectively. Asterisks represent significance by unpaired t-test for absolute changes in spike activity whereas significance in pie-chart of change in directionality in spiking is from Fisher's exact 2-tail test. The number of spikes per cell per 100 pA current injection increased with DBS at 10 Hz, 100 μsec and 2 V (B) and 3 V (C), but not at 1 V electrical stimulation (A). (For interpretation of the references to colour in this figure legend, the reader is referred to the web version of this article.)

little change in membrane potential or excitatory post-synaptic potentials (EPSPs) (Fig. 4ii).

With VL neurons, we observed similar effects from stimulation in the interface area between the VA and VL thalamic nuclei. With 1 V stimulation, VL neurons had 4.9 ± 1.6 more APs per cell with 100 pA positive current injection (n = 8 cells, p = 0.042, Fig. 6A) and 2 V

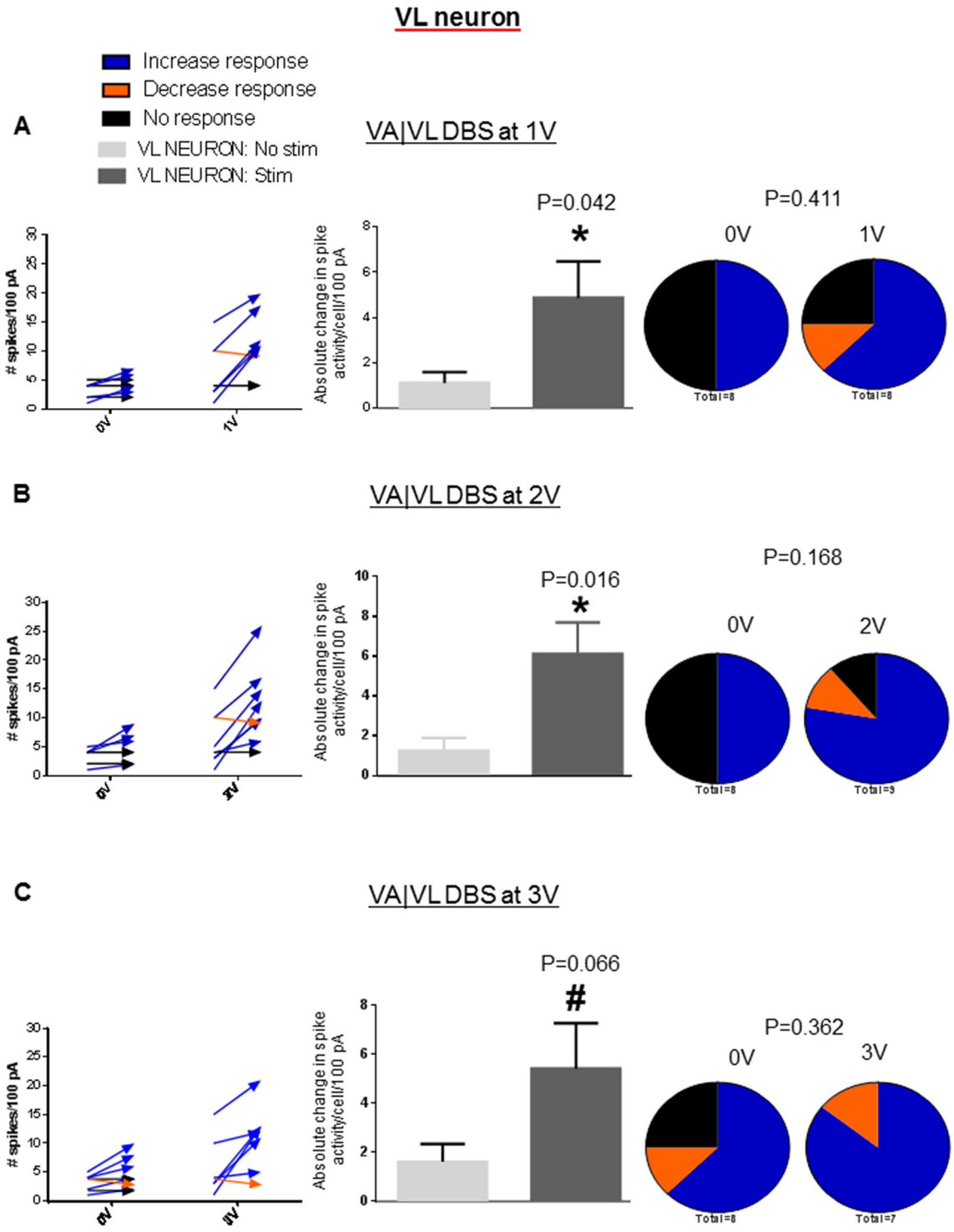

Fig. 6. Spiking activity of VL thalamic neurons before and during 1 V (A), 2 V (B), 3 V (C) stimulation in the VA|VL interface. Data shown for spikes elicited with 100 pA positive current injection. Beginning of arrows represent evoked response at baseline relative to endpoint, representing evoked response following 5 min baseline (0 V) or baseline plus 5 min stimulation (1, 2 or 3 V). The coinciding percentage change in the direction of the neuronal activity is shown as pie charts on the right with orange, blue and black denoting a decrease, increase or no change in spiking activity with stimulation, respectively. Asterisks represent significance by unpaired t-test for absolute changes in spike activity whereas significance in pie-chart of change in directionality in spiking is from Fisher's exact 2-tail test. The number of spikes per cell per 100 pA current injection increased with DBS at 10 Hz, 100 μsec and 1 V (A) and 2 V (B) with a trend towards significance at 3 V electrical stimulation (C) shown as a pound sign. (For interpretation of the references to colour in this figure legend, the reader is referred to the web version of this article.)

stimulation elicited 6.1 ± 1.6 more APs per cell (n = 9 cells, p = 0.016, Fig. 6B). With 3 V stimulation, there were 5.4 ± 1.9 more APs per cell per 100 pA positive current injection although significance was not reached (n = 7 cells, p = 0.066, Fig. 6C). As we had noted with VA neurons, the changes in hyper-excitability were not due to changes in resting membrane potential and input resistance at all voltages (data not shown). However, in contrast to VA neurons, the proportion of VL neurons with increased or decreased spiking activity with stimulation at any voltage did not change (Fig. 6A–C). Notably, the majority of VL neurons with evoked burst APs prior to VA|VL stimulation transitioned

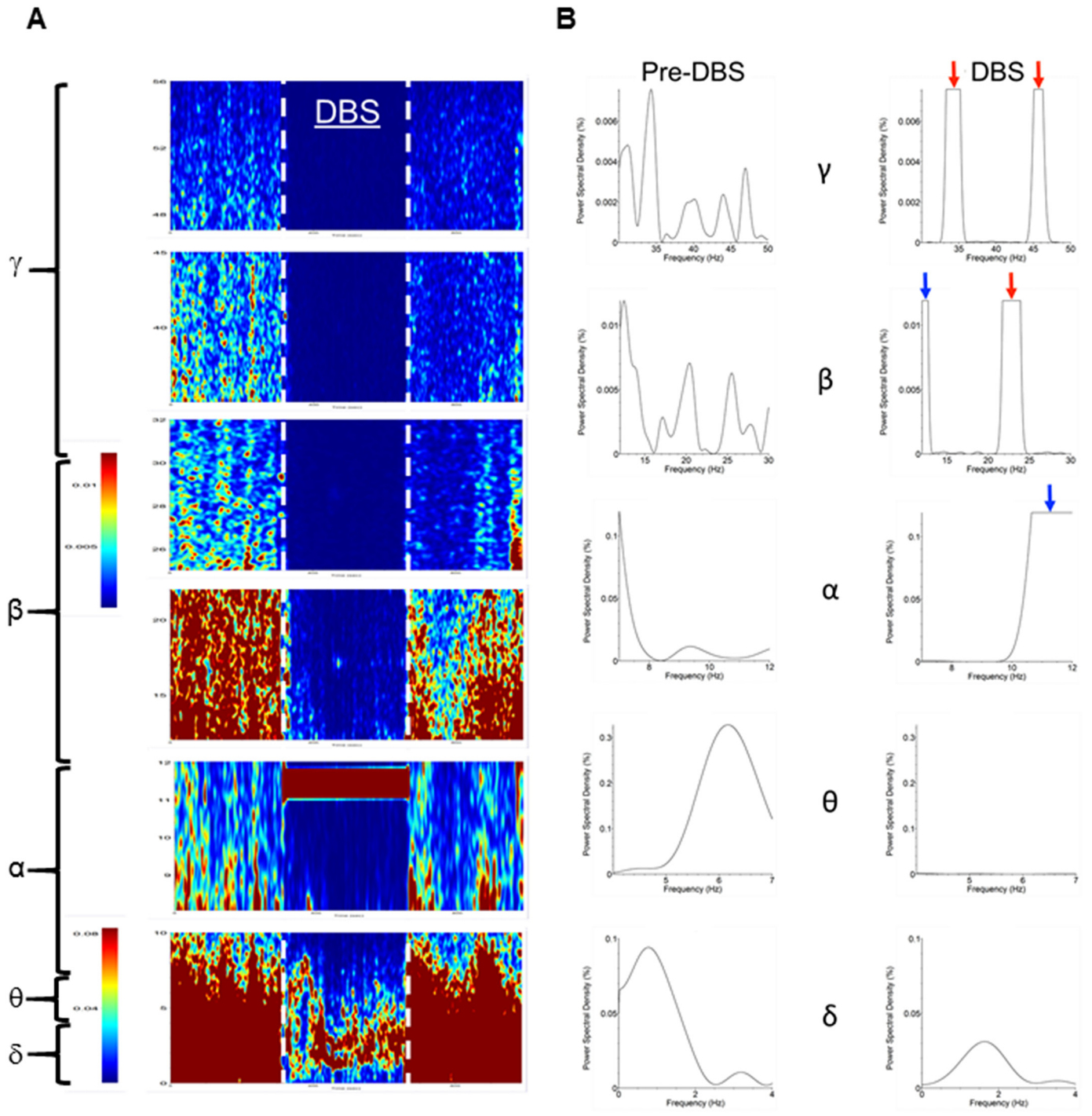

Fig. 7. Spectrogram analysis of local field potentials (LFPs) of M1 cortex before, during and after VA|VL stimulation show altered powers in various frequency domains spanning delta, theta, alpha, beta and gamma ranges. (A) is a spectrogram representative of the patterns observed in the aforementioned frequency domains before, during and after 2 VA|VL DBS sessions performed on each six PD rats. All of these are normalized to each other except for the delta frequency range (lowest panel) which exceeds limits. Therefore, heat scales are provided for the two different representations. (B) is a representative power spectral densities (PSDs) at each frequency domain from the same animal with blue arrows denoting the stimulation and red arrows representing harmonics in the PSD. (For interpretation of the references to colour in this figure legend, the reader is referred to the web version of this article.)

to many single spikes with stimulation ($p = 0.007$) (Fig. 4Bi). In passive current clamp mode, VA|VL electrical stimulation elicited large EPSPs that were time-locked to each other (Fig. 4Bii), which were not seen with VA neuronal recordings.

3.4. VA|VL DBS reduced oscillatory power in multiple frequency domains in the M1 cortex in PD rats

LFPs were monitored from the M1 cortex in PD rats while performing the LAT (n = 6 with two DBS sessions, Fig. 7A & B). Prior to stimulation, PD rats had dominant delta and beta oscillations (Fig. 7A). With VA|VL DBS, animals improved forelimb function with varied changes in the lower frequency domains and more consistent effects at

Table 1
Summary of changes in the % total of the power spectral density (PSD) from LFPs from the M1 cortex using a 1 min window from each individual VA|VL DBS session per PD rat for each frequency domain: delta (0–4 Hz), theta (4–8 Hz), alpha (8–12 Hz), beta (12–30 Hz) and gamma (> 30 Hz) frequencies. 'Up' indicates larger PSDs with DBS vs. with no stimulation; 'down' indicates lower PSDs whereas 'even' represents no change with or without VA|VL DBS. Stimulation and harmonics were excluded from analysis except at 10 Hz.

RAT ID & Session#	Delta (0-4 hz)	Theta (4-7 hz)	Alpha (8-12 hz)	Beta (12-30 hz)	Gamma (> 30 hz)
PDH38:DBS1	Down	Down	Down	Down	Down
PDH38:DBS2	Down	Down	Up	Down	Down
PDH49:DBS1	Up	Down	Up	Down	Down
PDH49:DBS2	Down	Down	Down	Down	Down
PDHSO:DBS1	Down	Even	Up	Even	Down
PDHSO:DBS2	Up	Down	Up	Down	Down
PDB7:DBS1	Down	Up	Up	Down	Down
PDB7:DBS2	Down	Down	Down	Down	Down
PDB9:DBS1	Down	Down	Up	Down	Down
PDB9:DBS2	Up	Down	Down	Down	Down
PDAC2:DBS1	Down	Down	Down	Down	Down
PDAC2:DBS2	Down	Down	Up	Down	Down
CHANGE (pre-DBS→DBS)					
Up	27.3%	9.1%	54.5%	0.0%	0.0%
Down	75.0%	83.3%	41.7%	91.7%	100.0%
Even	0.0%	8.3%	0.0%	8.3%	0.0%

the higher frequencies (Table 1). Specifically, delta frequencies increased and decreased in 25% and 75% of trials, respectively. For theta frequencies, 8.3% of trials (1/12) showed an increase or no change (1/12) but 83.3% (10/12) had a decrease in power. In the alpha frequency domain, 58.3% increased with VA|VL DBS whereas 41.7% of trials decreased, albeit increases may also arise from stimulation artifacts present throughout this entire frequency domain. More consistent responses were seen with beta and gamma frequencies. For the former, 91.7% decreased and 8.3% did not change. For the latter, 100% of trials showed a decrease in gamma frequencies in PD rats with improved performance in the LAT.

4. Discussion

In our study, we found that DBS at 10 Hz in the VA, VL or VA|VL improved forelimb akinesia in hemiparkinsonian 'PD' rats performing the LAT. Moreover, our in vitro and in vivo electrophysiological data suggest that increased excitability of VA and VL neurons and reduced oscillatory power in beta and gamma frequencies in the M1 cortex, respectively, may contribute to the underlying therapeutic mechanism.

DBS is now the preferred management strategy in PD patients with motor fluctuations and dyskinesia despite optimized pharmacotherapy and has revolutionized the way PD motor symptoms are managed today. Currently, the subthalamic nucleus (STN) and globus pallidus interna (GPi) are the two FDA-approved DBS targets for PD; both reside in the basal ganglia and are equally efficacious in treating motor dysfunction in PD (Durif et al., 2002; Liang et al., 2006; Moro et al., 2010) with beneficial effects lasting many years (Castrioto et al., 2011; Krack et al., 2003; Rodriguez-Oroz et al., 2005; Schupbach et al., 2005; Volkmann et al., 2009). Yet, its utility is limited to well-selected patients based on their levodopa responsiveness, age, physical and mental health, cognition and disease severity. Some individuals who are treated with DBS may also not benefit fully from this treatment due to stimulation-induced adverse effects, even after drug and stimulation readjustments are made (Castelli et al., 2010). Specifically, STN-DBS may worsen depression (Berney et al., 2002), hypomania (Mallet et al., 2007), decrease verbal fluency (Castelli et al., 2010; Morrison et al., 2004; York et al., 2008) or diminish cognitive performance (York et al., 2008) in PD patients. With GPi, the use of DBS in this area generally elicits similar, but less pronounced non-motor adverse effects as STN-DBS (Follett et al., 2010). For these reasons, current research endeavors are developing technologies in DBS targeting and imaging, electrical current steering to shape stimulation fields, parameter optimization algorithms, better metrics for identifying appropriate DBS patients and real-time dynamic control of stimulation such as closed-loop DBS.

While current DBS targets are being optimized, we investigate whether the motor thalamic nuclei, specifically the rat VA and VL motor thalamic nuclei, can serve as a novel effective target for DBS for PD in this study. The motor thalamus is well conserved across vertebrates (Bosch-Bouju et al., 2013) and contain primarily glutamatergic neurons with projections to motor cortices in specific cortical layers (Hooks et al., 2013; McFarland and Haber, 2002). A signature of these neurons is bursting APs due to T-type calcium channels (Huguenard and McCormick, 1992; Jahnsen and Llinas, 1984a, 1984b; McCormick and Huguenard, 1992). In rodents, the motor thalamus can be broadly divided as the VA and VL with the former receiving inhibitory GABAergic input from output BG nuclei (e.g., GPi rat homolog) and the latter receiving excitatory glutamate signaling from deep cerebellar nuclei efferents (Kuramoto et al., 2009). In primates, different characterization and nomenclature have historically been used to define this brain area, e.g. Hassler, Walker, Olszewski, Jones classifications (Hassler, 1950; Jones, 1981, 1990; Macchi and Jones, 1997) with areas receiving BG input denoted as the VA per se, but the VL subdivided in the anterior territory with various nomenclature such as the Voa, VLo and the Vop. Jone's classification describes this collectively as the VL anterior nucleus (VLa) (Jones, 1981, 1990). Here, the Voa is primarily innervated by the BG whereas the Vop receives some BG afferents, but mostly cerebellar innervation (Hassler et al., 1979; Ilinsky et al., 2018; Ilinsky and Kultas-Ilinsky, 2002; Krack et al., 2002; Kultas-Ilinsky et al., 2011; Macchi and Jones, 1997). The posterior territory of the VL is denoted as VL caudalis (VLc) or VL posterior (VLp), which can be further subdivided into the VL posterior lateral oralis (VPLo), also referred to as the ventral intermediate nucleus (Vim) (Hassler, 1950; Jones, 1981, 1990; Olszewski, 1952). Overall, there is distinct segregation of territories innervated by the BG and cerebellum in the motor thalamus (Ilinsky and Kultas-Ilinsky, 1987; Kuo and Carpenter, 1973; Kuramoto et al., 2009; Schell and Strick, 1984) with the VA in rat or the VA, Voa and rostral VLa in humans innervated by the former and the VL in rat or the caudal VLa, Vop, VLc and VLp/Vim in humans receiving cerebellar input.

Our study is the first to electrically stimulate this thalamic area for PD treatment although others have reported that neuromodulating the VA-VL thalamus at low or high stimulation frequencies can improve akinesia and dystonia, respectively. Specifically, DBS at 130 Hz of the Voa/VLa thalamus reduced head tremor by 78% and dystonia by 70% in patients with dystonia (Pauls et al., 2014) and optogenetic stimulation of the VA thalamus with theta bursts (5 pulses/s with 3 spikes/pulse) improved akinesia in a haloperidol-induced rat model of PD (Seeger-Armbruster et al., 2015). Whereas the VA and VL thalamus has been overlooked as a DBS target for PD, another thalamic nucleus called the ventralis intermedius (Vim) is FDA-approved for treatment of essential tremors (Pahwa et al., 2006; Ramirez-Zamora and Okun, 2016; Whiting et al., 2018).

Our in vitro recordings revealed that VL neurons transitioned from single evoked bursting action potentials to many single action potentials which may increase information fidelity from the BG to the motor cortex (Brown, 2007; Guo et al., 2008; Rubin et al., 2012) and mitigate abnormal bursting activity in the VL in PD patients (Magnin et al., 2000). Reduction in spontaneous thalamic rebound firing following inhibitory signaling from the rodent GPi was posited to underly motor deficits in the SPR-KO mouse model of PD (Kim et al., 2017). Here, we did not find differences in rebound burst APs between VA and VL neurons with VA|VL stimulation but did note that VL neurons transitioned from burst to single spiking APs and had large (> 8 mV)

depolarizing potentials time-locked to VA|VL stimulation; presumably due to stimulation-evoked glutamate release from cerebellar afferents. These were absent in VA neurons, which are innervated by BG output GABAergic terminals (data not shown) (Bosch-Bouju et al., 2013; Kuramoto et al., 2009; Nakamura et al., 2014). With that said, there are limitations in extrapolating whole-cell recording data obtained in brain slices from naïve non-PD rat pups having severed connections to motor cortices and absence of passage of fibers to improvements in LAT performance from DBS in hemiparkinsonian rats. Future studies can include single-unit recordings in these animals to delineate changes in neural signaling in vivo.

We speculate that DBS in the VA, VL and VA|VL improved motor function in PD rats via thalamic nuclei mono-synaptic innervation of motor-related cortices. For instance, VA thalamic neurons mostly innervating layer I of premotor, primary somatosensory and primary and secondary motor areas and in the striatum whereas VL neurons send their projections to layers II-V (Kuramoto et al., 2009; Yamamoto et al., 1990). DBS in the motor thalamic areas may increase neural activity in layer I (via the VA) in addition to layers II-V (via the VL) in the premotor, primary and secondary motor and primary supplemental cortices in vivo. This presumably stems from VA, VL or VA|VL DBS exciting both glutamatergic VA and VL neurons from current spread even with reciprocal excitatory innervation from cortical layer V and VI neurons onto VA and VL proximal and distal dendrites, respectively (Kakei et al., 2001; Kultas-Ilinsky et al., 2003; McFarland and Haber, 2002). Aside from affecting spike frequencies, our stimulation paradigm could also reduce burstiness and synchronization in motor cortices observed in PD (Goldberg et al., 2002; Parr-Brownlie and Hyland, 2005; Pasquereau and Turner, 2011). Yet, electrical fields also affect fibers of passage and adjacent brain structures (Chaturvedi et al., 2013; Gunalan et al., 2018; McIntyre and Grill, 2002). Therefore, changes in other brain areas could contribute to motor improvement with motor thalamic DBS such as cortical afferents in the motor thalamus that arise from collaterals from descending axons projecting to the brainstem and spinal cord. Lastly, our LFP data showed dominant beta oscillations in the M1 motor cortex which is consistent with other reports in PD (Brazhnik et al., 2012; Sharott et al., 2005; Tinkhauser et al., 2018; Williams et al., 2002). Notably, VA|VL DBS diminish these and gamma frequencies which contrasts with increase in gamma frequencies with levodopa and GPi or STN DBS (Kempf et al., 2009; Kuhn et al., 2017; McCairn and Turner, 2015; Silberstein et al., 2005; Weiss et al., 2015). It's plausible that VA and VL monosynaptic connections to motor cortices may lend direct modulation of motor function with DBS whereas neuromodulation of BG nuclei such as the STN and GPi are more influenced by dopaminergic tone.

Considering a more systems network explanation, the VA and VL thalamic complex has conventionally been viewed as a relay center for BG and cerebellar driven signals to the motor cortices (Albin et al., 1989; Alexander and Crutcher, 1990; Bar-Gad et al., 2003; DeLong, 1990). More recently, this notion has evolved to include an integrative function of these parallel motor systems, which may serve as a candidate site for neuromodulation to reassert normal fidelity in signal consolidation for normal movement (Guo et al., 2008; Rubin et al., 2012). Given that the BG is involved in motor learning and selection of motor plans (Barnes et al., 2005; Jog et al., 1999; McFarland and Haber, 2002; Redgrave et al., 2010; Xiao et al., 2009) whereas the cerebellum provides proprioceptive information from sensory afferents of the spinal cord and vestibular system for error signaling to coordinate movement (D'Angelo et al., 2011; Ebner et al., 2011; Horne and Butler, 1995), it's plausible that VA, VL or VA|VL DBS increases information and signal fidelity in the VA and VL, which consolidates the two parallel motor systems to improve PD motor symptoms.

Overall, our data suggests that motor thalamus DBS improves motor function in PD rats. Future experiments will bring to light whether this DBS target has less adverse effects than STN and GPi DBS. With that said, the VA, VL and VA|VL thalamic areas are more motor-related in connectivity with little associative and limbic functions (Hintzen et al., 2018; Kha et al., 2001; Kuramoto et al., 2009), which is in contrast to the STN (Parent and Hazrati, 1995; Temel et al., 2005). Albeit speculative, it suggests that DBS of the VA, VL and/or VA|VL could possibly mitigate concerns of cognitive impairment and depression from DBS, but this will require further investigation to substantiate this notion. Also, according to calculations for total energy delivered (Koss et al., 2005), VA-VL DBS requires 2 orders of magnitude less energy (1.39×10^{-7} V^2 x Hz x sec/Ω) than STN-DBS (2×10^{-5} V^2 x Hz x sec/Ω) (see supplemental material) to provide similar improvements to PD rats in the LAT. This posits that less battery replacement surgeries would be necessary, which has clear clinical merit since these are replaced every 3–4 year (Bin-Mahfoodh et al., 2003; van Riesen et al., 2016). This will lessen travel and operation obligations for PD patients visiting movement disorder clinics which can be many hours away and tiresome for individuals with motor dysfunction.

In conclusion, our findings posit that electrical stimulation of the VA, VL and the interface region between these motor thalamic nuclei (VA|VL) is a site amenable to neuromodulation for PD. Importantly, it sheds light on this critically situated brain area, which consolidates basal ganglia (BG) and cerebellar neurocircuitry, as a therapeutic foci and a relatively understudied node in the cortico-basal ganglia-thalamic network.

Acknowledgements

We would like to thank the DiNapoli Parkinson's Research Fund for supporting this study. ESM is supported by the Rily Family Chair in Parkinson's Disease.

Declaration of disclosures

Dr. Pilitsis consults for Boston Scientific and Medtronic and has grant support from Boston Scientific, Medtronic, Abbott, Jazz Pharmaceuticals and NIH 1R01CA166379 and NIH 1R43NS107076-01A1. She is also chief medical advisor for Centauri and has stock equity. Dr. Shin has industry support from General Electric Global Research. Dr. Molho consults for Neurocrine Biosciences, is a promotional speaker for Neurocrine Biosciences and receives grant support from Cure Huntington Disease Initiative/Huntington Study Group, Civitas Therapeutics, Michael J. Fox Foundation/Parkinson Study Group, Biogen, St. Jude Medical.

Appendix A. Supplementary data

Supplementary data to this article can be found online at https://doi.org/10.1016/j.expneurol.2019.03.008.

References

Albin, R.L., Young, A.B., Penney, J.B., 1989. The functional anatomy of basal ganglia disorders. Trends Neurosci. 12, 366–375.
Alexander, G.E., Crutcher, M.D., 1990. Functional architecture of basal ganglia circuits: neural substrates of parallel processing. Trends Neurosci. 13, 266–271.
Bar-Gad, I., Morris, G., Bergman, H., 2003. Information processing, dimensionality reduction and reinforcement learning in the basal ganglia. Prog. Neurobiol. 71, 439–473.
Barnes, T.D., Kubota, Y., Hu, D., Jin, D.Z., Graybiel, A.M., 2005. Activity of striatal neurons reflects dynamic encoding and recoding of procedural memories. Nature 437, 1158–1161.
Berney, A., Vingerhoets, F., Perrin, A., Guex, P., Villemure, J.G., Burkhard, P.R., Benkelfat, C., Ghika, J., 2002. Effect on mood of subthalamic DBS for Parkinson's disease: a consecutive series of 24 patients. Neurology 59, 1427–1429.
Bin-Mahfoodh, M., Hamani, C., Sime, E., Lozano, A.M., 2003. Longevity of batteries in internal pulse generators used for deep brain stimulation. Stereotact. Funct. Neurosurg. 80, 56–60.
Bosch-Bouju, C., Hyland, B.I., Parr-Brownlie, L.C., 2013. Motor thalamus integration of cortical, cerebellar and basal ganglia information: implications for normal and parkinsonian conditions. Front. Comput. Neurosci. 7, 163.
Brazhnik, E., Cruz, A.V., Avila, I., Wahba, M.I., Novikov, N., Ilieva, N.M., McCoy, A.J.,

Gerber, C., Walters, J.R., 2012. State-dependent spike and local field synchronization between motor cortex and substantia nigra in hemiparkinsonian rats. J. Neurosci. 32, 7869–7880.
Brown, P., 2007. Abnormal oscillatory synchronisation in the motor system leads to impaired movement. Curr. Opin. Neurobiol. 17, 656–664.
Buhmann, C., Huckhagel, T., Engel, K., Gulberti, A., Hidding, U., Poetter-Nerger, M., Goerendt, I., Ludewig, P., Braass, H., Choe, C.U., Krajewski, K., Oehlwein, C., Mittmann, K., Engel, A.K., Gerloff, C., Westphal, M., Koppen, J.A., Moll, C.K.E., Hamel, W., 2017. Adverse events in deep brain stimulation: a retrospective long-term analysis of neurological, psychiatric and other occurrences. PLoS ONE 12, e0178984.
Castelli, L., Rizzi, L., Zibetti, M., Angrisano, S., Lanotte, M., Lopiano, L., 2010. Neuropsychological changes 1-year after subthalamic DBS in PD patients: a prospective controlled study. Parkinsonism Relat. Disord. 16, 115–118.
Castrioto, A., Lozano, A.M., Poon, Y.Y., Lang, A.E., Fallis, M., Moro, E., 2011. Ten-year outcome of subthalamic stimulation in Parkinson disease: a blinded evaluation. Arch. Neurol. 68, 1550–1556.
Chaturvedi, A., Lujan, J.L., McIntyre, C.C., 2013. Artificial neural network based characterization of the volume of tissue activated during deep brain stimulation. J. Neural Eng. 10, 056023.
Chen, H., Burton, E.A., Ross, G.W., Huang, X., Savica, R., Abbott, R.D., Ascherio, A., Caviness, J.N., Gao, X., Gray, K.A., Hong, J.S., Kamel, F., Jennings, D., Kirshner, A., Lawler, C., Liu, R., Miller, G.W., Nussbaum, R., Peddada, S.D., Rick, A.C., Ritz, B., Siderowf, A.D., Tanner, C.M., Troster, A.I., Zhang, J., 2013. Research on the premotor symptoms of Parkinson's disease: clinical and etiological implications. Environ. Health Perspect. 121, 1245–1252.
D'Angelo, E., Mazzarello, P., Prestori, F., Mapelli, J., Solinas, S., Lombardo, P., Cesana, E., Gandolfi, D., Congi, L., 2011. The cerebellar network: from structure to function and dynamics. Brain Res. Rev. 66, 5–15.
DeBusk, B.C., DeBruyn, E.J., Snider, R.K., Kabara, J.F., Bonds, A.B., 1997. Stimulus-dependent modulation of spike burst length in cat striate cortical cells. J. Neurophysiol. 78, 199–213.
DeLong, M.R., 1990. Primate models of movement disorders of basal ganglia origin. Trends Neurosci. 13, 281–285.
Durif, F., Lemaire, J.J., Debilly, B., Dordain, G., 2002. Long-term follow-up of globus pallidus chronic stimulation in advanced Parkinson's disease. Mov. Disord. 17, 803–807.
Ebner, T.J., Hewitt, A.L., Popa, L.S., 2011. What features of limb movements are encoded in the discharge of cerebellar neurons? Cerebellum 10, 683–693.
Escola, S., Fontanini, A., Katz, D., Paninski, L., 2011. Hidden Markov models for the stimulus-response relationships of multistate neural systems. Neural Comput. 23, 1071–1132.
Fabbrini, G., Brotchie, J.M., Grandas, F., Nomoto, M., Goetz, C.G., 2007. Levodopa-induced dyskinesias. Mov. Disord. 22, 1379–1389 (quiz 1523).
Follett, K.A., Weaver, F.M., Stern, M., Hur, K., Harris, C.L., Luo, P., Marks Jr., W.J., Rothlind, J., Sagher, O., Moy, C., Pahwa, R., Burchiel, K., Hogarth, P., Lai, E.C., Duda, J.E., Holloway, K., Samii, A., Horn, S., Bronstein, J.M., Stoner, G., Starr, P.A., Simpson, R., Baltuch, G., De Salles, A., Huang, G.D., Reda, D.J., 2010. Pallidal versus subthalamic deep-brain stimulation for Parkinson's disease. N. Engl. J. Med. 362, 2077–2091.
Garcia, L., Audin, J., D'Alessandro, G., Bioulac, B., Hammond, C., 2003. Dual effect of high-frequency stimulation on subthalamic neuron activity. J. Neurosci. 23, 8743–8751.
Goldberg, J.A., Boraud, T., Maraton, S., Haber, S.N., Vaadia, E., Bergman, H., 2002. Enhanced synchrony among primary motor cortex neurons in the 1-methyl-4-phenyl-1,2,3,6-tetrahydropyridine primate model of Parkinson's disease. J. Neurosci. 22, 4639–4653.
Gunalan, K., Howell, B., McIntyre, C.C., 2018. Quantifying axonal responses in patient-specific models of subthalamic deep brain stimulation. Neuroimage 172, 263–277.
Guo, Y., Rubin, J.E., McIntyre, C.C., Vitek, J.L., Terman, D., 2008. Thalamocortical relay fidelity varies across subthalamic nucleus deep brain stimulation protocols in a data-driven computational model. J. Neurophysiol. 99, 1477–1492.
Hassler, R., 1950. Die Anatomie des Thalamus. Archiv fur Psychiatrie und Nervenkrankheiten, vereinigt mit Zeitschrift fur die gesamte Neurologie und Psychiatrie. 184. pp. 3–4.
Hassler, R., Mundinger, F., Riechert, T., 1979. Stereotaxis in Parkinson Syndrome : Clinical-Anatomical Contributions to its Pathophysiology. Springer, Berlin.
Hintzen, A., Pelzer, E.A., Tittgemeyer, M., 2018. Thalamic interactions of cerebellum and basal ganglia. Brain Struct. Funct. 223, 569–587.
Hooks, B.M., Mao, T., Gutnisky, D.A., Yamawaki, N., Svoboda, K., Shepherd, G.M., 2013. Organization of cortical and thalamic input to pyramidal neurons in mouse motor cortex. J. Neurosci. 33, 748–760.
Horne, M.K., Butler, E.G., 1995. The role of the cerebello-thalamo-cortical pathway in skilled movement. Prog. Neurobiol. 46, 199–213.
Huguenard, J.R., McCormick, D.A., 1992. Simulation of the currents involved in rhythmic oscillations in thalamic relay neurons. J. Neurophysiol. 68, 1373–1383.
Ilinsky, I.A., Kultas-Ilinsky, K., 1987. Sagittal cytoarchitectonic maps of the Macaca mulatta thalamus with a revised nomenclature of the motor-related nuclei validated by observations on their connectivity. J. Comp. Neurol. 262, 331–364.
Ilinsky, I.A., Kultas-Ilinsky, K., 2002. Motor thalamic circuits in primates with emphasis on the area targeted in treatment of movement disorders. Mov. Disord. 17 (Suppl. 3), S9–14.
Ilinsky, I., Horn, A., Paul-Gilloteaux, P., Gressens, P., Verney, C., Kultas-Ilinsky, K., 2018. Human motor thalamus reconstructed in 3D from continuous sagittal sections with identified subcortical afferent territories. eNeuro 5.
Jahnsen, H., Llinas, R., 1984a. Electrophysiological properties of Guinea-pig thalamic neurones: an in vitro study. J. Physiol. 349, 205–226.
Jahnsen, H., Llinas, R., 1984b. Ionic basis for the electro-responsiveness and oscillatory properties of Guinea-pig thalamic neurones in vitro. J. Physiol. 349, 227–247.
Jog, M.S., Kubota, Y., Connolly, C.I., Hillegaart, V., Graybiel, A.M., 1999. Building neural representations of habits. Science 286, 1745–1749.
Jones, E.G., 1981. Functional subdivision and synaptic organization of the mammalian thalamus. Int. Rev. Physiol. 25, 173–245.
Jones, E.G., 1990. Correlation and revised nomenclature of ventral nuclei in the thalamus of human and monkey. Stereotact. Funct. Neurosurg. 54 (55), 1–20.
Kakei, S., Na, J., Shinoda, Y., 2001. Thalamic terminal morphology and distribution of single corticothalamic axons originating from layers 5 and 6 of the cat motor cortex. J. Comp. Neurol. 437, 170–185.
Kempf, F., Brucke, C., Salih, F., Trottenberg, T., Kupsch, A., Schneider, G.H., Doyle Gaynor, L.M., Hoffmann, K.T., Vesper, J., Wohrle, J., Altenmuller, D.M., Krauss, J.K., Mazzone, P., Di Lazzaro, V., Yelnik, J., Kuhn, A.A., Brown, P., 2009. Gamma activity and reactivity in human thalamic local field potentials. Eur. J. Neurosci. 29, 943–953.
Kha, H.T., Finkelstein, D.I., Tomas, D., Drago, J., Pow, D.V., Horne, M.K., 2001. Projections from the substantia nigra pars reticulata to the motor thalamus of the rat: single axon reconstructions and immunohistochemical study. J. Comp. Neurol. 440, 20–30.
Kim, J., Kim, Y., Nakajima, R., Shin, A., Jeong, M., Park, A.H., Jeong, Y., Jo, S., Yang, S., Park, H., Cho, S.H., Cho, K.H., Shim, I., Chung, J.H., Paik, S.B., Augustine, G.J., Kim, D., 2017. Inhibitory basal ganglia inputs induce excitatory motor signals in the thalamus. Neuron 95, 1181–1196 e1188.
Koss, A.M., Alterman, R.L., Tagliati, M., Shils, J.L., 2005. Calculating total electrical energy delivered by deep brain stimulation systems. Ann. Neurol. 58, 168 (author reply 168-169).
Krack, P., Dostrovsky, J., Ilinsky, I., Kultas-Ilinsky, K., Lenz, F., Lozano, A., Vitek, J., 2002. Surgery of the motor thalamus: problems with the present nomenclatures. Mov. Disord. 17 (Suppl. 3), S2–S8.
Krack, P., Batir, A., Van Blercom, N., Chabardes, S., Fraix, V., Ardouin, C., Koudsie, A., Limousin, P.D., Benazzouz, A., LeBas, J.F., Benabid, A.L., Pollak, P., 2003. Five-year follow-up of bilateral stimulation of the subthalamic nucleus in advanced Parkinson's disease. N. Engl. J. Med. 349, 1925–1934.
Kuhn, J., Haumesser, J.K., Beck, M.H., Altschuler, J., Kuhn, A.A., Nikulin, V.V., van Riesen, C., 2017. Differential effects of levodopa and apomorphine on neuronal population oscillations in the cortico-basal ganglia loop circuit in vivo in experimental parkinsonism. Exp. Neurol. 298, 122–133.
Kultas-Ilinsky, K., Sivan-Loukianova, E., Ilinsky, I.A., 2003. Reevaluation of the primary motor cortex connections with the thalamus in primates. J. Comp. Neurol. 457, 133–158.
Kultas-Ilinsky, K., Ilinsky, I.A., Verney, C., 2011. Glutamic acid decarboxylase isoform 65 immunoreactivity in the motor thalamus of humans and monkeys: gamma-aminobutyric acidergic connections and nuclear delineations. J. Comp. Neurol. 519, 2811–2837.
Kuo, J.S., Carpenter, M.B., 1973. Organization of pallidothalamic projections in the rhesus monkey. J. Comp. Neurol. 151, 201–236.
Kuramoto, E., Furuta, T., Nakamura, K.C., Unzai, T., Hioki, H., Kaneko, T., 2009. Two types of thalamocortical projections from the motor thalamic nuclei of the rat: a single neuron-tracing study using viral vectors. Cereb. Cortex 19, 2065–2077.
Liang, G.S., Chou, K.L., Baltuch, G.H., Jaggi, J.L., Loveland-Jones, C., Leng, L., Maccarone, H., Hurtig, H.I., Colcher, A., Stern, M.B., Kleiner-Fisman, G., Simuni, T., Siderowf, A.D., 2006. Long-term outcomes of bilateral subthalamic nucleus stimulation in patients with advanced Parkinson's disease. Stereotact. Funct. Neurosurg. 84, 221–227.
Lundblad, M., Andersson, M., Winkler, C., Kirik, D., Wierup, N., Cenci, M.A., 2002. Pharmacological validation of behavioural measures of akinesia and dyskinesia in a rat model of Parkinson's disease. Eur. J. Neurosci. 15, 120–132.
Macchi, G., Jones, E.G., 1997. Toward an agreement on terminology of nuclear and subnuclear divisions of the motor thalamus. J. Neurosurg. 86, 670–685.
Magnin, M., Morel, A., Jeanmonod, D., 2000. Single-unit analysis of the pallidum, thalamus and subthalamic nucleus in parkinsonian patients. Neuroscience 96, 549–564.
Mallet, L., Schupbach, M., N'Diaye, K., Remy, P., Bardinet, E., Czernecki, V., Welter, M.L., Pelissolo, A., Ruberg, M., Agid, Y., Yelnik, J., 2007. Stimulation of subterritories of the subthalamic nucleus reveals its role in the integration of the emotional and motor aspects of behavior. Proc. Natl. Acad. Sci. U. S. A. 104, 10661–10666.
McCairn, K.W., Turner, R.S., 2015. Pallidal stimulation suppresses pathological dysrhythmia in the parkinsonian motor cortex. J. Neurophysiol. 113, 2537–2548.
McCormick, D.A., Huguenard, J.R., 1992. A model of the electrophysiological properties of thalamocortical relay neurons. J. Neurophysiol. 68, 1384–1400.
McFarland, N.R., Haber, S.N., 2002. Thalamic relay nuclei of the basal ganglia form both reciprocal and nonreciprocal cortical connections, linking multiple frontal cortical areas. J. Neurosci. 22, 8117–8132.
McIntyre, C.C., Grill, W.M., 2002. Extracellular stimulation of central neurons: influence of stimulus waveform and frequency on neuronal output. J. Neurophysiol. 88, 1592–1604.
Moro, E., Lozano, A.M., Pollak, P., Agid, Y., Rehncrona, S., Volkmann, J., Kulisevsky, J., Obeso, J.A., Albanese, A., Hariz, M.I., Quinn, N.P., Speelman, J.D., Benabid, A.L., Fraix, V., Mendes, A., Welter, M.L., Houeto, J.L., Cornu, P., Dormont, D., Tornqvist, A.L., Ekberg, R., Schnitzler, A., Timmermann, L., Wojtecki, L., Gironell, A., Rodriguez-Oroz, M.C., Guridi, J., Bentivoglio, A.R., Contarino, M.F., Romito, L., Scerrati, M., Janssens, M., Lang, A.E., 2010. Long-term results of a multicenter study on subthalamic and pallidal stimulation in Parkinson's disease. Mov. Disord. 25, 578.586.
Morrison, C.E., Borod, J.C., Perrine, K., Beric, A., Brin, M.F., Rezai, A., Kelly, P., Sterio, D., Germano, I., Weisz, D., Olanow, C.W., 2004. Neuropsychological functioning following bilateral subthalamic nucleus stimulation in Parkinson's disease. Arch. Clin.

Neuropsychol. 19, 165–181.
Nakamura, K.C., Sharott, A., Magill, P.J., 2014. Temporal coupling with cortex distinguishes spontaneous neuronal activities in identified basal ganglia-recipient and cerebellar-recipient zones of the motor thalamus. Cereb. Cortex 24, 81–97.
O'Connor, K.A., Feustel, P.J., Ramirez-Zamora, A., Molho, E., Pilitsis, J.G., Shin, D.S., 2016. Investigation of diazepam efficacy on anxiety-like behavior in hemiparkinsonian rats. Behav. Brain Res. 301, 226–237.
O'Connor, K.A., Mahoney, E., Ramirez-Zamora, A., Molho, E.S., Pilitsis, J.G., Shin, D.S., 2017. Effect of diazepam and yohimbine on neuronal activity in sham and hemiparkinsonian rats. Neuroscience 351, 71–83.
Olszewski, J., 1952. The Thalamus of the *Macaca mulatta* an Atlas for Use with the Stereotaxic Instrument. Karger, Basel.
Pahwa, R., Lyons, K.E., Wilkinson, S.B., Simpson Jr., R.K., Ondo, W.G., Tarsy, D., Norregaard, T., Hubble, J.P., Smith, D.A., Hauser, R.A., Jankovic, J., 2006. Long-term evaluation of deep brain stimulation of the thalamus. J. Neurosurg. 104, 506–512.
Parent, A., Hazrati, L.N., 1995. Functional anatomy of the basal ganglia. II. The place of subthalamic nucleus and external pallidum in basal ganglia circuitry. Brain Res. Brain Res. Rev. 20, 128–154.
Parr-Brownlie, L.C., Hyland, B.I., 2005. Bradykinesia induced by dopamine D2 receptor blockade is associated with reduced motor cortex activity in the rat. J. Neurosci. 25, 5700–5709.
Pasquereau, B., Turner, R.S., 2011. Primary motor cortex of the parkinsonian monkey: differential effects on the spontaneous activity of pyramidal tract-type neurons. Cereb. Cortex 21, 1362–1378.
Pauls, K.A., Hammesfahr, S., Moro, E., Moore, A.P., Binder, E., El Majdoub, F., Fink, G.R., Sturm, V., Krauss, J.K., Maarouf, M., Timmermann, L., 2014. Deep brain stimulation in the ventrolateral thalamus/subthalamic area in dystonia with head tremor. Mov. Disord. 29, 953–959.
Paxinos, G., Watson, C., 1996. The Rat Brain in Stereotaxic Coordinates. Academic Pres, San Diego (Compact 3rd ed).
Phookan, S., Sutton, A.C., Walling, I., Smith, A., O'Connor, K.A., Campbell, J.C., Calos, M., Yu, W., Pilitsis, J.G., Brotchie, J.M., Shin, D.S., 2015. Gap junction blockers attenuate beta oscillations and improve forelimb function in hemiparkinsonian rats. Exp. Neurol. 265, 160–170.
Postuma, R.B., Berg, D., Stern, M., Poewe, W., Olanow, C.W., Oertel, W., Obeso, J., Marek, K., Litvan, I., Lang, A.E., Halliday, G., Goetz, C.G., Gasser, T., Dubois, B., Chan, P., Bloem, B.R., Adler, C.H., Deuschl, G., 2015. MDS clinical diagnostic criteria for Parkinson's disease. Mov. Disord. 30, 1591–1601.
Ramirez-Zamora, A., Okun, M.S., 2016. Deep brain stimulation for the treatment of uncommon tremor syndromes. Expert. Rev. Neurother. 16, 983–997.
Redgrave, P., Rodriguez, M., Smith, Y., Rodriguez-Oroz, M.C., Lehericy, S., Bergman, H., Agid, Y., DeLong, M.R., Obeso, J.A., 2010. Goal-directed and habitual control in the basal ganglia: implications for Parkinson's disease. Nat. Rev. Neurosci. 11, 760–772.
Rodriguez-Oroz, M.C., Obeso, J.A., Lang, A.E., Houeto, J.L., Pollak, P., Rehncrona, S., Kulisevsky, J., Albanese, A., Volkmann, J., Hariz, M.I., Quinn, N.P., Speelman, J.D., Guridi, J., Zamarbide, I., Gironell, A., Molet, J., Pascual-Sedano, B., Pidoux, B., Bonnet, A.M., Agid, Y., Xie, J., Benabid, A.L., Lozano, A.M., Saint-Cyr, J., Romito, L., Contarino, M.F., Scerrati, M., Fraix, V., Van Blercom, N., 2005. Bilateral deep brain stimulation in Parkinson's disease: a multicentre study with 4 years follow-up. Brain 128, 2240–2249.
Rubin, J.E., McIntyre, C.C., Turner, R.S., Wichmann, T., 2012. Basal ganglia activity patterns in parkinsonism and computational modeling of their downstream effects. Eur. J. Neurosci. 36, 2213–2228.
Schallert, T., Fleming, S.M., Leasure, J.L., Tillerson, J.L., Bland, S.T., 2000. CNS plasticity and assessment of forelimb sensorimotor outcome in unilateral rat models of stroke, cortical ablation, parkinsonism and spinal cord injury. Neuropharmacology 39, 777–787.
Schell, G.R., Strick, P.L., 1984. The origin of thalamic inputs to the arcuate premotor and supplementary motor areas. J. Neurosci. 4, 539–560.
Schupbach, W.M., Chastan, N., Welter, M.L., Houeto, J.L., Mesnage, V., Bonnet, A.M., Czernecki, V., Maltete, D., Hartmann, A., Mallet, L., Pidoux, B., Dormont, D., Navarro, S., Cornu, P., Mallet, A., Agid, Y., 2005. Stimulation of the subthalamic nucleus in Parkinson's disease: a 5 year follow up. J. Neurol. Neurosurg. Psychiatry 76, 1640–1644.
Seeger-Armbruster, S., Bosch-Bouju, C., Little, S.T., Smither, R.A., Hughes, S.M., Hyland, B.I., Parr-Brownlie, L.C., 2015. Patterned, but not tonic, optogenetic stimulation in motor thalamus improves reaching in acute drug-induced parkinsonian rats. J. Neurosci. 35, 1211–1216.
Sharott, A., Magill, P.J., Harnack, D., Kupsch, A., Meissner, W., Brown, P., 2005. Dopamine depletion increases the power and coherence of beta-oscillations in the cerebral cortex and subthalamic nucleus of the awake rat. Eur. J. Neurosci. 21, 1413–1422.
Shin, D.S., Carlen, P.L., 2008. Enhanced Ih depresses rat entopeduncular nucleus neuronal activity from high-frequency stimulation or raised Ke+. J. Neurophysiol. 99, 2203–2219.
Shin, D.S., Samoilova, M., Cotic, M., Zhang, L., Brotchie, J.M., Carlen, P.L., 2007. High frequency stimulation or elevated K+ depresses neuronal activity in the rat entopeduncular nucleus. Neuroscience 149, 68–86.
Silberstein, P., Pogosyan, A., Kuhn, A.A., Hotton, G., Tisch, S., Kupsch, A., Dowsey-Limousin, P., Hariz, M.I., Brown, P., 2005. Cortico-cortical coupling in Parkinson's disease and its modulation by therapy. Brain 128, 1277–1291.
Spillantini, M.G., Crowther, R.A., Jakes, R., Hasegawa, M., Goedert, M., 1998. Alpha-Synuclein in filamentous inclusions of Lewy bodies from Parkinson's disease and dementia with lewy bodies. Proc. Natl. Acad. Sci. U. S. A. 95, 6469–6473.
Sutton, A.C., Yu, W., Calos, M.E., Mueller, L.E., Berk, M., Shim, J., Molho, E.S., Brotchie, J.M., Carlen, P.L., Shin, D.S., 2013a. Elevated potassium provides an ionic mechanism for deep brain stimulation in the hemiparkinsonian rat. Eur. J. Neurosci. 37, 231–241.
Sutton, A.C., Yu, W., Calos, M.E., Smith, A.B., Ramirez-Zamora, A., Molho, E.S., Pilitsis, J.G., Brotchie, J.M., Shin, D.S., 2013b. Deep brain stimulation of the substantia nigra pars reticulata improves forelimb akinesia in the hemiparkinsonian rat. J. Neurophysiol. 109, 363–374.
Sutton, A.C., O'Connor, K.A., Pilitsis, J.G., Shin, D.S., 2015. Stimulation of the subthalamic nucleus engages the cerebellum for motor function in parkinsonian rats. Brain Struct. Funct. 220, 3595–3609.
Temel, Y., Blokland, A., Steinbusch, H.W., Visser-Vandewalle, V., 2005. The functional role of the subthalamic nucleus in cognitive and limbic circuits. Prog. Neurobiol. 76, 393–413.
Tinkhauser, G., Torrecillos, F., Duclos, Y., Tan, H., Pogosyan, A., Fischer, P., Carron, R., Welter, M.L., Karachi, C., Vandenberghe, W., Nuttin, B., Witjas, T., Regis, J., Azulay, J.P., Eusebio, A., Brown, P., 2018. Beta burst coupling across the motor circuit in Parkinson's disease. Neurobiol. Dis. 117, 217–225.
Tritsch, N.X., Rodriguez-Contreras, A., Crins, T.T., Wang, H.C., Borst, J.G., Bergles, D.E., 2010. Calcium action potentials in hair cells pattern auditory neuron activity before hearing onset. Nat. Neurosci. 13, 1050–1052.
Tysnes, O.B., Storstein, A., 2017. Epidemiology of Parkinson's disease. J. Neural Transm. 1996 (124), 901–905 Vienna, Austria.
van Riesen, C., Tsironis, G., Gruber, D., Klostermann, F., Krause, P., Schneider, G.H., Kupsch, A., 2016. Disease-specific longevity of impulse generators in deep brain stimulation and review of the literature. J. Neural Transm. (Vienna) 123, 621–630.
Volkmann, J., Albanese, A., Kulisevsky, J., Tornqvist, A.L., Houeto, J.L., Pidoux, B., Bonnet, A.M., Mendes, A., Benabid, A.L., Fraix, V., Van Blercom, N., Xie, J., Obeso, J., Rodriguez-Oroz, M.C., Guridi, J., Schnitzler, A., Timmermann, L., Gironell, A.A., Molet, J., Pascual-Sedano, B., Rehncrona, S., Moro, E., Lang, A.C., Lozano, A.M., Bentivoglio, A.R., Scerrati, M., Contarino, M.F., Romito, L., Janssens, M., Agid, Y., 2009. Long-term effects of pallidal or subthalamic deep brain stimulation on quality of life in Parkinson's disease. Mov. Disord. 24, 1154–1161.
Weiss, D., Klotz, R., Govindan, R.B., Scholten, M., Naros, G., Ramos-Murguialday, A., Bunjes, F., Meisner, C., Plewnia, C., Kruger, R., Gharabaghi, A., 2015. Subthalamic stimulation modulates cortical motor network activity and synchronization in Parkinson's disease. Brain 138, 679–693.
Whiting, B.B., Whiting, A.C., Whiting, D.M., 2018. Thalamic deep brain stimulation. Prog. Neurol. Surg. 33, 198–206.
Wichmann, T., Delong, M.R., 2011. Deep-Brain Stimulation for Basal Ganglia Disorders. Basal Ganglia. 1. pp. 65–77.
Wichmann, T., DeLong, M.R., 2016. Deep brain stimulation for movement disorders of basal ganglia origin: restoring function or functionality? Neurotherapeutics 13, 264–283.
Wijesinghe, R., Solomon, S.G., Camp, A.J., 2013. Noise normalizes firing output of mouse lateral geniculate nucleus neurons. PLoS ONE 8, e57961.
Williams, D., Tijssen, M., Van Bruggen, G., Bosch, A., Insola, A., Di Lazzaro, V., Mazzone, P., Oliviero, A., Quartarone, A., Speelman, H., Brown, P., 2002. Dopamine-dependent changes in the functional connectivity between basal ganglia and cerebral cortex in humans. Brain 125, 1558–1569.
Xiao, D., Zikopoulos, B., Barbas, H., 2009. Laminar and modular organization of prefrontal projections to multiple thalamic nuclei. Neuroscience 161, 1067–1081.
Yamamoto, T., Kishimoto, Y., Yoshikawa, H., Oka, H., 1990. Cortical laminar distribution of rat thalamic ventrolateral fibers demonstrated by the PHA-L anterograde labeling method. Neurosci. Res. 9, 148–154.
York, M.K., Dulay, M., Macias, A., Levin, H.S., Grossman, R., Simpson, R., Jankovic, J., 2008. Cognitive declines following bilateral subthalamic nucleus deep brain stimulation for the treatment of Parkinson's disease. J. Neurol. Neurosurg. Psychiatry 79, 789–795.
Yu, W., Walling, I., Smith, A.B., Ramirez-Zamora, A., Pilitsis, J.G., Shin, D.S., 2016. Deep brain stimulation of the ventral pallidum attenuates epileptiform activity and seizing behavior in pilocarpine-treated rats. Brain Stimul. 9, 285–295.